

# Ge-rich SiGe-on-insulator for waveguide optical modulator application fabricated by Ge condensation and SiGe regrowth

Younghyun Kim,<sup>1,\*</sup> Masafumi Yokoyama,<sup>1</sup> Noriyuki Taoka,<sup>1</sup> Mitsuru Takenaka,<sup>1,2</sup> and Shinichi Takagi<sup>1</sup>

<sup>1</sup>*Dept. of Electrical Engineering and Information Systems, The University of Tokyo 7-3-1 Hongo, Bunkyo-ku, Tokyo 113-0032, Japan*

<sup>2</sup>*PRESTO, JST, 4-1-8 Honcho Kawaguchi, Saitama 332-0012, Japan*

*\*yhkim@mosfet.t.u-tokyo.ac.jp*

**Abstract:** We have numerically analyzed plasma dispersion effect in a Ge-rich SiGe layer for optical modulator applications. Since strain induces reduction in effective masses of electron and hole, we expect enhanced plasma dispersion effect in a strained Ge-rich SiGe layer. The plasma dispersion effects of Si<sub>0.15</sub>Ge<sub>0.85</sub> on Si<sub>0.2</sub>Ge<sub>0.8</sub> for hole and electron are expected to be approximately 3.0 and 1.5 times larger than those of Si. To realize Ge-rich SiGe-based waveguide optical modulators, we have also investigated the fabrication procedure of SiGe-on-insulator (SGOI) wafers. We have successfully fabricated Ge-rich SGOI wafers without any thick SiGe buffer layers by using Ge condensation in conjunction with the SiGe regrowth technique. We have evaluated the SGOI by Raman spectroscopy, atomic force microscopy (AFM), reflected high energy electron diffraction (RHEED) and transmission electron microscopy (TEM). Ge-rich SiGe waveguides have been fabricated on the SGOI wafer. The propagation loss was found to be approximately 13 dB/mm, which can be reduced to be below 2 dB/mm by optimizing the Ge condensation process. We expect that strained SiGe grown on the fabricated SGOI exhibits more than 2.3 times higher plasma dispersion than Si in case of a carrier injection type, suitable for high-performance waveguide optical modulators.

©2013 Optical Society of America

**OCIS codes:** (130.3120) Integrated optics devices; (250.7360) Waveguide modulators.

---

## References and links

1. A. Liu and M. Paniccia, "Advances in silicon photonic devices for silicon-based optoelectronic applications," *Physica E* **35**(2), 223–228 (2006).
2. International Technology Roadmap for Semiconductors, (2011 Edition). Available: <http://www.itrs.net/Links/2011ITRS/2011Chapters/2011Interconnect.pdf>
3. L. Liao, D. Samara-Rubio, M. Morse, A. Liu, D. Hodge, D. Rubin, U. D. Keil, and T. Franck, "High speed silicon Mach-Zehnder modulator," *Opt. Express* **13**(8), 3129–3135 (2005).
4. L. Liao, A. Liu, D. Rubin, J. Basak, Y. Chetrit, H. Nguyen, R. Cohen, N. Izhaky, and M. Paniccia, "40 Gbit/s silicon optical modulator for high-speed applications," *Electron. Lett.* **43**(22), 1196–1197 (2007).
5. F. Y. Gardes, D. J. Thomson, N. G. Emerson, and G. T. Reed, "40 Gb/s silicon photonics modulator for TE and TM polarisations," *Opt. Express* **13**(8), 3129–3135 (2005).
6. Q. Xu, B. Schmidt, S. Pradhan, and M. Lipson, "Micrometre-scale silicon electro-optic modulator," *Nature* **435**(7040), 325–327 (2005).
7. P. Dong, R. Shafiiha, S. Liao, H. Liang, N.-N. Feng, D. Feng, G. Li, X. Zheng, A. V. Krishnamoorthy, and M. Asghari, "Wavelength-tunable silicon microring modulator," *Opt. Express* **18**(11), 10941–10946 (2010).
8. H. C. Nguyen, Y. Sakai, M. Shinkawa, N. Ishikura, and T. Baba, "Photonic crystal silicon optical modulators: carrier-injection and depletion at 10 Gb/s," *IEEE J. Quantum Electron.* **48**(2), 210–220 (2012).
9. M. Takenaka and S. Takagi, "Strain engineering of plasma dispersion effect for SiGe optical modulators," *IEEE J. Sel. Top. Quantum Electron.* **48**(1), 8–16 (2012).
10. M. V. Fischetti and S. E. Laux, "Band structure, deformation potentials, and carrier mobility in strained Si, Ge, and SiGe alloys," *J. Appl. Phys.* **80**(4), 2234–2252 (1996).

11. K. C. Saraswat, C. O. Chui, D. Kim, T. Krishnamohan, and A. Pethe, "High mobility materials and novel device structures for high performance nanoscale MOSFETs," *Electron Devices Meeting, 2006. IEDM '06. International*.
12. M. Oehme, J. Werner, O. Kirfel, and E. Kasper, "MBE growth of SiGe with high Ge content for optical applications," *Appl. Surf. Sci.* **254**(19), 6238–6241 (2008).
13. T. Tezuka, N. Sugiyama, T. Mizuno, M. Suzuki, and S. Takagi, "A Novel fabrication of ultrathin and relaxed SiGe buffer layers with high Ge fraction for sub-100 nm strained silicon-on-insulator MOSFETs," *Jpn. J. Appl. Phys.* **40**(Part 1, No. 4B), 2866–2874 (2001).
14. T. Tezuka, N. Sugiyama, T. Mizuno, M. Suzuki, and S. Takagi, "Ultrathin body SiGe-on-insulator pMOSFETs with high-mobility SiGe surface channels," *IEEE Trans. Electron. Dev.* **50**(5), 1328–1333 (2003).
15. S. Nakaharai, T. Tezuka, N. Sugiyama, Y. Moriyama, and S. Takagi, "Characterization of 7-nm-thick strained Ge-on-insulator layer fabricated by Ge-condensation technique," *Appl. Phys. Lett.* **83**(17), 3516–3518 (2003).
16. S. Balakumar, S. Peng, K. M. Hoe, G. Q. Lo, R. Kumar, N. Balasubramanian, D. L. Kwong, Y. L. Foo, and S. Tripathy, "Fabrication of thick SiGe on insulator ( $\text{Si}_{0.2}\text{Ge}_{0.8}\text{OI}$ ) by condensation of SiGe/Si superlattice grown on silicon on insulator," *Appl. Phys. Lett.* **90**(19), 192113 (2007).
17. S. Koh, K. Sawano, Y. Shiraki, N. Usami, K. Nakajima, X. Huang, and S. Uda, "Fabrication of p-i-n  $\text{Si}_{0.5}\text{Ge}_{0.5}$  photodetectors on SiGe-on-Insulator Substrates," 2004 first IEEE International Conference on Group IV Photonics.
18. R. A. Soref and B. R. Bennett, "Electrooptical effects in silicon," *IEEE J. Sel. Top. Quantum Electron.* **23**(1), 123–129 (1987).
19. R. Braunstein, A. R. Moore, and F. Herman, "Intrinsic optical absorption in germanium-silicon alloys," *Phys. Rev.* **109**(3), 695–710 (1958).
20. M. M. Rieger and P. Vogl, "Electronic-band parameters in strained  $\text{Si}_{1-x}\text{Ge}_x$  alloys on  $\text{Si}_{1-y}\text{Ge}_y$  substrates," *Phys. Rev. B Condens. Matter* **48**(19), 14276–14287 (1993).
21. D. V. Lang, R. People, J. C. Bean, and A. M. Sergent, "Measurement of the band gap of  $\text{Ge}_x\text{Si}_{1-x}/\text{Si}$  strained-layer heterostructures," *Appl. Phys. Lett.* **47**(12), 1333–1335 (1985).
22. F. Pezzoli, E. Bonera, E. Grilli, M. Guzzi, S. Sanguinetti, D. Chrastina, G. Isella, H. von Kañnel, E. Wintersberger, J. Stangl, and G. Bauer, "Raman spectroscopy determination of composition and strain in  $\text{Si}_{1-x}\text{Ge}_x/\text{Si}$  heterostructures," *Mat. Sci. in Semi. Proc.* **11**, 279–284 (2008).
23. S. W. Bedell, K. Fogel, D. K. Sadana, and H. Chen, "Defects and strain relaxation in silicon-germanium-on-insulator formed by high-temperature oxidation," *Appl. Phys. Lett.* **85**(24), 5869–5871 (2004).
24. Y. Zhang, K. Cai, C. Li, S. Chen, H. Lai, and J. Kang, "Strain relaxation in ultrathin SGOI substrates fabricated by multistep Ge condensation method," *J. Electrochem. Soc.* **156**(2), H115–H118 (2009).
25. N. Hirashita, Y. Moriyama, S. Nakaharai, T. Irisawa, N. Sugiyama, and S. Takagi, "Deformation induced holes in Ge-rich SiGe-on-insulator and Ge-on-insulator substrates fabricated by Ge condensation process," *Appl. Phys. Express* **1**, 101401 (2008).
26. Y. Moriyama, N. Hirashita, K. Usuda, S. Nakaharai, N. Sugiyama, E. Toyoda, and S. Takagi, "Study of the surface cleaning of GOI and SGOI substrates for Ge epitaxial growth," *Appl. Surf. Sci.* **256**(3), 823–829 (2009).
27. J. Humlicek, F. Lukes, and E. Schmidt, "Silicon-germanium alloys ( $\text{Si}_x\text{Ge}_{1-x}$ )," in *Handbook of Optical Constants of Solids II*, E. D. Palik, Ed. (Academic, 1991), pp. 607–636.
28. H. J. Stein, "Neutron-and proton-induced defects in SiGe alloys: optical absorption," *J. Appl. Phys.* **45**(5), 1954–1961 (1974).
29. T. Tezuka, S. Nakaharai, Y. Moriyama, N. Sugiyama, and S. Takagi, "High-mobility strained SiGe-on-insulator pMOSFETs with Ge-rich surface channels fabricated by local condensation technique," *IEEE Electron Device Lett.* **26**(4), 243–245 (2005).

## 1. Introduction

Convergence of photonics and electronics is one the most promising candidates of breakthrough on recent arising interconnection problems of complementary metal-oxide-semiconductor (CMOS) large-scale integrated (LSI) circuits in terms of bandwidth and power dissipation. Si photonics has especially attracted great attentions as a technology enabling an on-chip optical interconnection in LSIs for breaking the trade-off between the bandwidth and the power consumption of interconnections beyond the current copper interconnect technology [1,2]. A Si optical modulator is one of the fundamental building blocks for on-chip optical interconnections in Si LSIs. Recently, the high speed optical modulators have been demonstrated using a Mach-Zehnder interferometer (MZI) consisting of two 3-dB couplers and phase-shifters in which the refractive index is modulated through the plasma dispersion effect in Si. However, the device footprints, especially in terms of the length of phase-shifter of Si MZI modulators are several mm-lengths not enough for large integration in LSIs because of the weak plasma dispersion effect in Si [3–5].

To reduce the device footprint of the Si modulators, some resonance cavity structures including ring resonators [6,7] and photonic crystals [8] have been reported. However, the enhancement of the plasma dispersion effect itself is still required for further reduction in the

device footprint. For this purpose, we have predicted that strained silicon-germanium (SiGe) exhibits higher plasma dispersion effect than Si owing to the reduction in the conductivity mass induced by strain [9]. In electronics, it is well known that the effective mass of hole in SiGe alloy becomes lighter with increases in the Ge mole fraction and compressive strain, contributing high-mobility p-MOS transistors [10,11]. The fact can be applied not only for an electronic device but also for an optical modulator. The device footprints are expected to be reduced by enhancing the plasma dispersion effect by means of using light effective-mass of carriers in SiGe because the plasma dispersion effect is inversely proportional to the effective mass of a material according to the Drude model [9]. Additionally, the conductivity effective mass of electron can be also reduced by using Ge-rich SiGe with the Ge fraction larger than 85% because the high Ge fraction in SiGe induces the minimum conduction band transition from  $\Delta$  to  $L$  valley with the Ge-like light effective mass for electron. Therefore, Ge-rich SiGe-on-insulator is a promising material to achieve small device footprint with the high modulation efficiency for optical modulators.

However, the large lattice constant mismatch between Si and Ge makes it difficult to grow Ge-rich SiGe directly on Si without a thick buffer layer which are not suited for the integration with waveguides [12]. To overcome this problem, the Ge condensation method has been considered as the promising candidate, enabling the Ge-rich SiGe-on-insulator (SGOI) wafer without any buffer layers. Ge condensation was originally reported in [13] to form thin SGOI and Ge-on-insulator for SiGe or Ge-based metal-oxide-semiconductor field effect transistors (MOSFETs) [14,15] which are expected to replace conventional Si MOSFETs in logic circuit applications. For the MOSFET application, the thickness of SiGe or Ge is typically less than 10 nm to suppress the short channel effect. However such a thin SiGe layer is not suitable for optical applications.

The 250-nm-thick  $\text{Si}_{0.2}\text{Ge}_{0.8}$ -on-insulator has been reported so far by using Ge condensation in conjunction with intermixing annealing [16]. However, the Ge condensation of the thick SiGe layer makes it difficult to achieve a proper Ge fraction and strain value simultaneously for optical modulation applications. On the other hand, the  $\text{Si}_{0.5}\text{Ge}_{0.5}$ -on-insulator for a photodetector has been reported by using Ge condensation and  $\text{Si}_{0.5}\text{Ge}_{0.5}$  regrowth [17], which is also suitable for optical modulators because of its flexibility in Ge fraction and strain of a SiGe layer.

In this study, we have analyzed plasma dispersion effect in strained Ge-rich SiGe by using the Drude model for optical modulator application. We have also fabricated the 190-nm-thick  $\text{Si}_{0.2}\text{Ge}_{0.8}$ -on-insulator for waveguide optical modulators by using the Ge condensation technique in conjunction with the SiGe regrowth technique. The fabricated SiGe-on-insulator layer has been evaluated by Raman spectroscopy, atomic-force microscopy (AFM), and Hall measurement. We have also fabricated  $\text{Si}_{0.2}\text{Ge}_{0.8}$ -on-insulator photonic-wire waveguides to evaluate its propagation loss. The theoretical analyses on enhancement of the plasma dispersion effect in Ge-rich SiGe grown on the SiGe template fabricated by Ge condensation are also discussed for optical modulator applications.

## 2. Enhancement on plasma dispersion effect in Ge-rich SiGe layer

The plasma dispersion effect is expressed by the Drude model, which is mainly a function of free-carrier densities. The change in the refractive index ( $\Delta n$ ) is expressed by

$$\Delta n = -\frac{e^2 \lambda^2}{8\pi^2 c^2 \epsilon_0 n} \left( \frac{\Delta N_e}{m_{ce}^*} + \frac{\Delta N_h}{m_{ch}^*} \right) \quad (1)$$

where  $e$  is the electronic charge,  $\epsilon_0$  is the permittivity in vacuum,  $c$  is the speed of light in vacuum,  $\lambda$  is the wavelength of light,  $n$  is the unperturbed refractive index,  $m_{ce}^*$  and  $m_{ch}^*$  are the conductivity effective mass for electron and hole respectively [18].

As described equations by the Drude model, the change in the refractive index is inversely proportional to the conductivity effective mass. Therefore, the change in the refractive index is expected to be enhanced by reducing conductivity effective mass of carriers. It has been

predicted that the light hole conductivity mass in compressively strained  $\text{Si}_{0.5}\text{Ge}_{0.5}$  grown on Si can enhance MOS-based modulators [9]. However, it is necessary to reduce effective masses of electron as well as hole for *pin*-junction-based optical modulations in which both electrons and holes contribute the plasma dispersion effect for refractive index modulation.

Since the energy band structure of SiGe transits from the Si-like to the Ge-like structure when the Ge fraction is larger than approximately 85%, electron occupation is expected to become larger in the *L* valleys contributing lighter effective mass of electron [19]. Figure 1(a) shows the conductivity effective masses of electron and hole as a function of the Ge mole fraction in  $\text{Si}_{1-x}\text{Ge}_x$  grown on  $\text{Si}_{0.2}\text{Ge}_{0.8}$ . The conductivity effective mass of electron parallel to the surface (001) is taken from [20]. When biaxial strain is applied to (001) surface of SiGe, we can ignore anisotropy in the in-plane conductivity mass near the  $\Gamma$  point. Since we consider only TE-polarized light which has an electrical field only in (001) plane, the (001) in-plane conductivity effective mass was only taken into account in Eq. (1). Then conductivity hole mass was calculated by the *k-p* method as depicted in [17]. As shown in Fig. 1, the mass of hole decreases with an increase in the Ge fraction owing to compressive strain in SiGe.

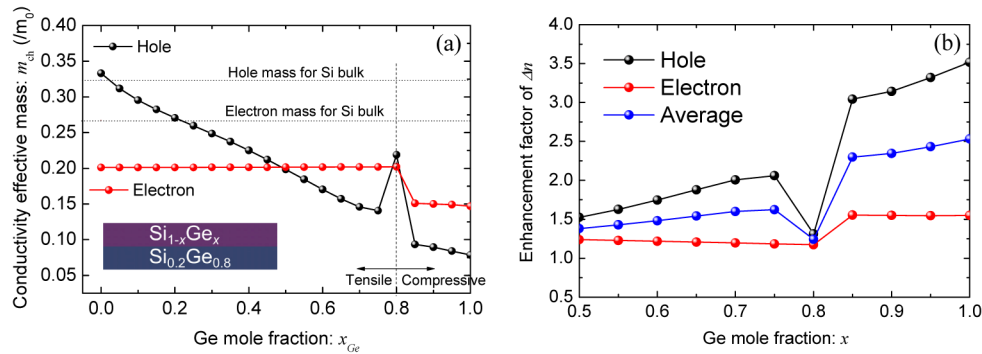


Fig. 1. (a) Conductivity effective masses of  $\text{Si}_{1-x}\text{Ge}_x$  on  $\text{Si}_{0.2}\text{Ge}_{0.8}$  as a function of Ge mole fraction. (b) Enhancement factors of change in refractive index of  $\text{Si}_{1-x}\text{Ge}_x$  on  $\text{Si}_{0.2}\text{Ge}_{0.8}$  as a function of Ge mole fraction.

The enhancement of the plasma dispersion effect in  $\text{Si}_{1-x}\text{Ge}_x$  on  $\text{Si}_{0.2}\text{Ge}_{0.8}$  was calculated by Eq. (1) as shown in Fig. 1(b). Since the conductivity effective masses for electron and hole rapidly decrease when the Ge fraction is larger than 80%, the enhancement of changes in the refractive index for electron and hole also show the rapid increase. The higher Ge mole fraction gives the larger enhancement, while the Ge fraction less than 85% is reasonable for the waveguide-modulator owing to the band-to-band absorption of the narrowed bandgap [21]. Consequently, the plasma dispersion effects of  $\text{Si}_{0.15}\text{Ge}_{0.85}$  on  $\text{Si}_{0.2}\text{Ge}_{0.8}$  for hole and electron are expected to be approximately 3.0 and 1.5 times larger, and the average of the enhancement of electron and hole is 2.3 times larger than those of Si considering a *pin* carrier injection type due to carrier neutrality condition.

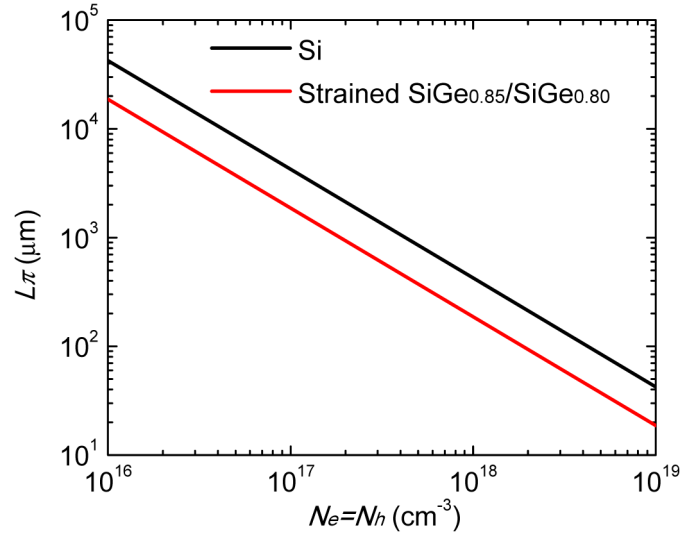


Fig. 2. Length required  $\pi$ -phase shift as a function of carrier density.

Figure 2 shows the length of the Ge-rich SiGe phase shifter required for  $\pi$ -phase shift as a function of carrier density injected through a *pin* junction. It is found in Fig. 2 that the device length of strained SiGe can be less than a half of the conventional Si device. When injected electron and hole density is  $1 \times 10^{18} \text{ cm}^{-3}$ , the lengths of phase shifter are approximately 190  $\mu\text{m}$  in case of the Ge-rich SiGe device.

### 3. Fabrication of Ge-rich SiGe-on-insulator by Ge condensation and SiGe regrowth

The SGOI substrate was prepared from a commercially available (001) Si-on-insulator (SOI) substrate by Ge condensation and SiGe regrowth without any thick buffer layers as shown in Fig. 3. First, a SOI layer (Si = 160 nm, buried oxide layer (BOX) = 2  $\mu\text{m}$ ) was thinned to be 15 nm by thermal oxidation at 1100  $^\circ\text{C}$  and buffered HF etching of the top  $\text{SiO}_2$  layer. Then, a 40-nm-thick pseudomorphic  $\text{Si}_{0.7}\text{Ge}_{0.3}$  layer and a 8-nm-thick Si cap layer were grown by molecular beam epitaxy (MBE) in Fig. 3(a). After the growth, Ge condensation was carried out by thermal oxidation at the temperatures of lower than the melting point of the SiGe. During thermal oxidation, the Si atoms were selectively oxidized and the Ge atoms were condensed in the remained SiGe layer in Fig. 3(b). Thus, the 11-nm-thick  $\text{Si}_{0.2}\text{Ge}_{0.8}$  layer was obtained on the BOX in Fig. 3(c). Finally, after removing the  $\text{SiO}_2$  layers and cleaning the thin SGOI wafer,  $\text{Si}_{0.19}\text{Ge}_{0.81}$  (175 nm) was grown on the Ge-condensed SGOI substrate by MBE in Fig. 3(d). We expect that one of the optimal structures for carrier-injection type optical modulators is a relaxed  $\text{SiGe}_{0.80}$ /Ge-rich  $\text{SiGe}_{x>0.80}$ /relaxed  $\text{SiGe}_{0.80}$ -OI double hetero structure as shown in Fig. 1. Thus, we have fabricated the relaxed  $\text{SiGe}_{0.80}$ -OI structure to evaluate fundamental properties of relaxed  $\text{SiGe}_{0.80}$  which is important to understand properties of the  $\text{SiGe}_{0.80}$ /Ge-rich  $\text{SiGe}_{x>0.80}$ /  $\text{SiGe}_{0.80}$ -OI structure.

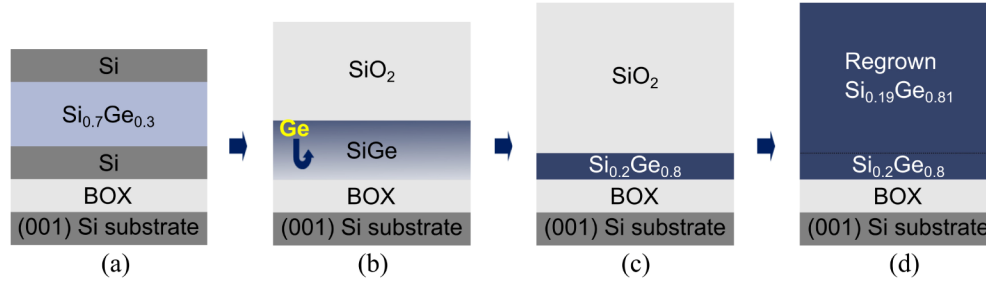


Fig. 3. Fabrication flow of Ge-rich SGOI by Ge condensation and SiGe regrowth technique: (a) Growth of Si<sub>0.7</sub>Ge<sub>0.3</sub> on SOI, (b) Ge condensation by thermal annealing (c) Formation of 11-nm-thick Si<sub>0.2</sub>Ge<sub>0.8</sub>-on-insulator structure by Ge condensation, and (d) Regrowth of Si<sub>0.19</sub>Ge<sub>0.81</sub> (175 nm) on SGOI substrate by MBE.

#### 4. Evaluation of the Ge-rich SiGe-on-insulator

We have evaluated the fabricated Ge-rich SGOI to clarify its properties by using Raman spectroscopy, AFM, and Hall measurement. Figure 4 shows the Raman spectra of the SGOI (Ge = 28, 56, 65, and 80%) during Ge condensation and the SGOI (Ge = 81%) after the SiGe regrowth. The Ge fractions and strain values in the SiGe alloys were determined by the Raman spectra [22]. During Ge condensation, the compressive strain gradually increased with an increase in the Ge fraction of 28% to 65%. However, it decreased with the Ge fraction larger than 60 – 65% due to strain relaxation. On the other hands, the Ge peak of regrown SGOI evidently shifted to left side, which is almost same value of the relaxed Ge peak of SiGe alloys. Thus, the fully-relaxed Ge-rich SGOI was obtained by regrowth without any thick buffer layers.

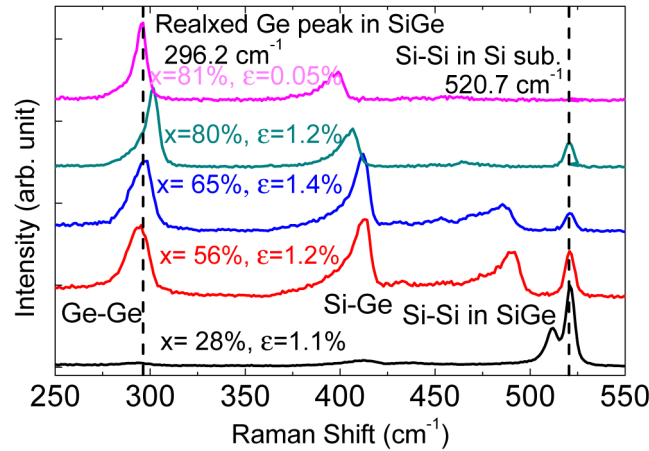


Fig. 4. Raman spectra of SGOI (Ge = 28, 56, 65, and 80%) during Ge condensation and SGOI (Ge = 81%) after SiGe regrowth.

Figures 5 show the root-mean-square ( $R_{rms}$ ) of surface roughness evaluated by AFM and the *in situ* reflection high energy electron diffraction (RHEED) images with [110] direction of the as-grown Si<sub>0.7</sub>Ge<sub>0.3</sub>-OI, Ge-condensed Si<sub>0.2</sub>Ge<sub>0.8</sub>-OI, and regrown Si<sub>0.19</sub>Ge<sub>0.81</sub>-OI, respectively. In general, during Ge condensation, the strain relaxation related to defect generation causes surface roughening [23,24]. Although  $R_{rms}$  was increased by Ge condensation, the surface roughness was alleviated by regrowth. The RHEED pattern of the Ge-condensed Si<sub>0.19</sub>Ge<sub>0.81</sub>-OI in Fig. 5(e) shows a spotty ( $1 \times 1$ ) pattern which indicates 3-dimensional island morphology whereas the pattern of the regrown Si<sub>0.19</sub>Ge<sub>0.81</sub>-OI in Fig. 5(f)

shows longish ( $2 \times 1$ ) pattern which indicates that the crystal quality was improved by the regrowth process.

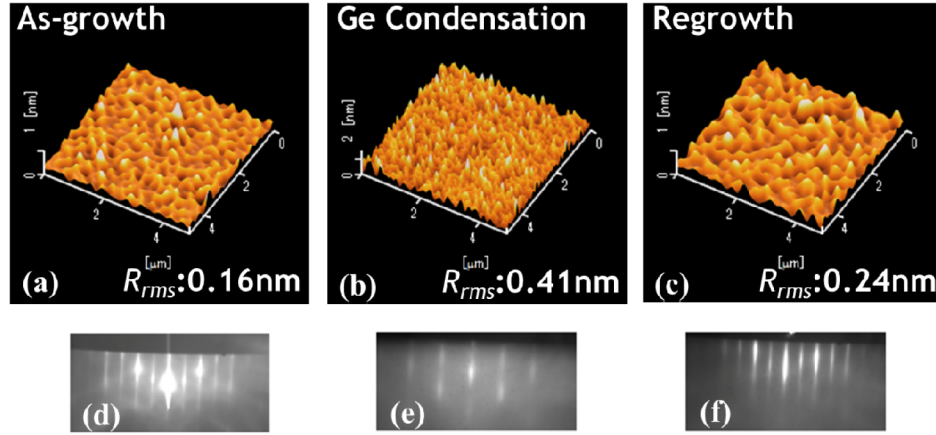


Fig. 5. Surface roughness of three samples measured by AFM and RHEED patterns of (a) and (d) as-grown  $\text{Si}_{0.7}\text{Ge}_{0.3}\text{-OI}$ , (b) and (e) Ge-condensed  $\text{Si}_{0.2}\text{Ge}_{0.8}\text{-OI}$ , and (c) and (f) Regrown  $\text{Si}_{0.2}\text{Ge}_{0.8}\text{-OI}$ .

The hole concentrations in the SiGe layers after Ge condensation and SiGe regrowth have been investigated by Hall measurement as summarized in Table 1. As discussed in Ref. [25], the defect generation during Ge condensation causes undesirable high hole concentration. After Ge condensation, the condensed SiGe layer exhibits high hole concentration of  $2.8 \times 10^{18} \text{ cm}^{-3}$ , while the hole concentration of the SGOI including the condensed SiGe and regrown SiGe layers is reduced to be  $9.5 \times 10^{17} \text{ cm}^{-3}$  after regrowth. From these results, the hole concentration of the regrown SiGe layer is expected to be  $7.6 \times 10^{17} \text{ cm}^{-3}$ .

**Table 1. Hole concentrations of the Ge-condensed SiGe layer, and the Ge-condensed SiGe + regrown SiGe layers, and the regrown SiGe layer evaluated by Hall measurement.**

	Ge condensed SiGe layer	Ge-condensed SiGe + regrown SiGe layers	Regrown SiGe layer
Hole concentration ( $\text{cm}^{-3}$ )	$2.8 \times 10^{18}$	$9.5 \times 10^{17}$	$7.6 \times 10^{17}$

Figures 6 show cross-sectional transmission electron microscopy (TEM) images. It is observed in Figs. 6 that several dislocations are extended from the dislocations of the SiGe layer formed during Ge condensation. Although the boundary between the condensed  $\text{Si}_{0.2}\text{Ge}_{0.8}\text{-OI}$  and regrown  $\text{Si}_{0.19}\text{Ge}_{0.81}$  layer points up the necessities of improvements of the wet pre-epitaxy treatment before the regrowth, the further improvement in the SiGe crystal quality can be obtained by optimizing the Ge condensation process for reducing the threading dislocations [26].



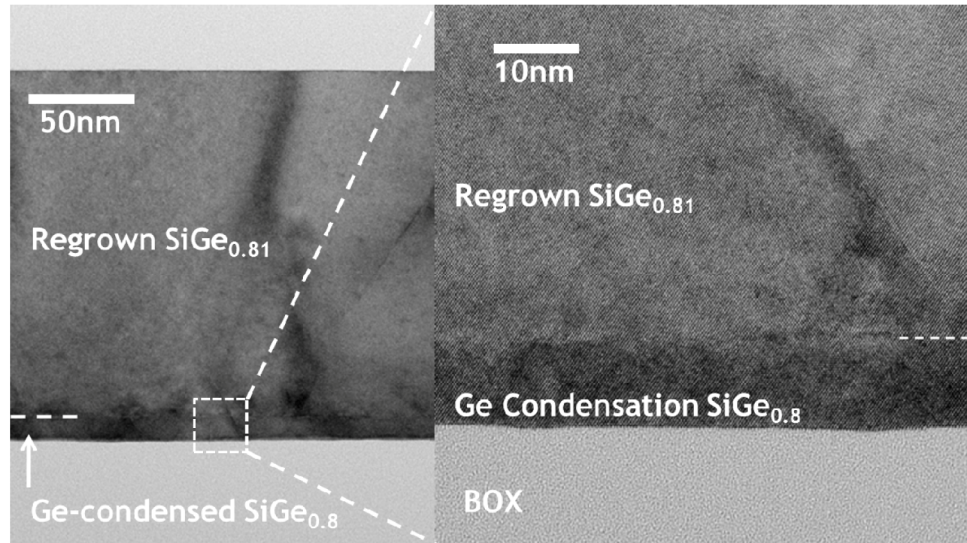


Fig. 6. Cross-sectional TEM images of SGOI formed by Ge condensation and SiGe regrowth.

### 5. Propagation loss of Ge-rich SiGe-on-insulator photonic-wire waveguide

The SiGe waveguide was fabricated using the SGOI substrate to evaluate the propagation loss. A 50-nm-thick SiO<sub>2</sub> hard mask was deposited on the SGOI by plasma-enhanced chemical vapor deposition (PECVD). After patterning, the hard mask and SiGe layer were etched by reactive ion etching. Then, a 500-nm-thick SiO<sub>2</sub> was deposited by PECVD for passivation. Finally, the handle wafer of SGOI was polished as thick as 300  $\mu\text{m}$  to cleave the patterned sample. A schematic of the fabricated waveguide is shown in the inset of Fig. 7.

The propagation loss of straight waveguides was measured by the cut-back method. As shown in Fig. 7, the loss of the fabricated SGOI waveguide is approximately 13 dB/mm at wavelength of 1.55  $\mu\text{m}$ , whereas the loss of the reference SOI waveguide is  $\sim 1$  dB/mm. Since the reference SOI waveguide exhibits much smaller propagation loss than the SGOI waveguide, we expect that the propagation loss caused by the line-edge roughness (LER) of the mesa or the line-width fluctuation (LWF) is negligible in our experiments. The high propagation loss mainly arises from several factors including the absorption of the high Ge fraction and the free-carrier absorption by the high hole density of  $7.6 \times 10^{17} \text{ cm}^{-3}$  in the SiGe layer. The absorption coefficient of SiGe with the Ge fraction of 80% is approximately 2 – 4  $\text{cm}^{-1}$  [27], thus the propagation loss from the band-to-band absorption of the SiGe layer is approximately 0.8 – 2 dB/mm. The propagation loss from the free-carrier absorption in the SiGe layer is estimated to be around 2 – 5 dB/mm according to the Drude model. The residual propagation loss of 5 – 9 dB/mm is expected from the absorption due to the crystal dislocations in the SiGe layer [28]. Therefore, the propagation loss from the free-carrier absorption and the crystal dislocations can be improved by optimizing the fabrication procedure of Ge-rich SiGe-on-insulator. We expect that the defect density in a condensed SiGe layer can be reduced by using Ge condensation at higher temperature close to the melting point of SiGe. Although the propagation loss of the Ge-rich SiGe waveguide is expected to be still high for passive waveguides even after optimizing the Ge condensation and regrowth condition, we can use the local Ge condensation technique reported in Ref. [29] to reduce the propagation loss in passive regions. By using the local Ge condensation technique in conjunction with selective area regrowth, we can monolithically integrate a Ge-rich SiGe layer for active regions and a low-Ge-content SiGe or a Si layer for passive regions. Thus, we can avoid additional propagation loss in the passive area.



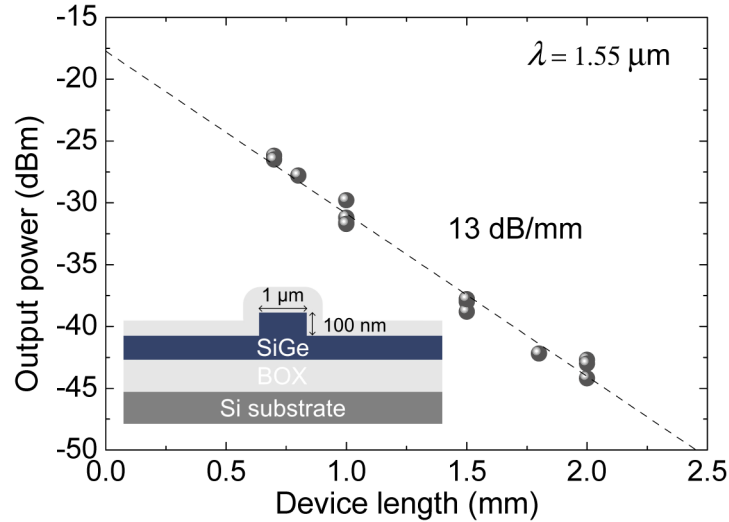


Fig. 7. Propagation loss of straight waveguides fabricated on SGOI. SGOI waveguides with the width of 1  $\mu\text{m}$  and with the length of 0.7 - 2.0 mm. Here, the propagation loss was estimated using the wavelength of 1.55  $\mu\text{m}$ .

## 6. Conclusion

We have investigated plasma dispersion effect in Ge-rich SiGe for the application of optical modulators. According to the Drude model, the enhancement factors of plasma dispersion effects for hole and electron in  $\text{Si}_{0.15}\text{Ge}_{0.85}$  on  $\text{Si}_{0.2}\text{Ge}_{0.8}$  are expected to be approximately 3.0 and 1.5, respectively. We have investigated the fabrication procedure of Ge-rich SGOI wafer by using the Ge condensation and regrowth techniques for waveguide optical modulator applications. The 186-nm-thick Ge-rich  $\text{Si}_{0.19}\text{Ge}_{0.81}$ -on-insulator was successfully fabricated without any thick buffer layers. Although the propagation loss of the Ge-rich SGOI photonic-wire waveguide is 13 dB/mm which is much higher than that of the conventional SOI waveguides, the propagation loss is expected to be reduced down to be less than 2 dB/mm by further optimizing Ge condensation. The strained SiGe layer grown on the fabricated SGOI exhibits 2.3 times higher plasma dispersion than Si in case of a carrier injection type. We also expect that the fabrication process of Ge-rich SGOI investigated in this paper can be applied to grow Ge/SiGe multi quantum well (MQW) structure for modulator and laser diode applications. Therefore, the presented CMOS compatible fabrication process of Ge-rich SGOI based on the Ge condensation and regrowth technique is highly promising for high-performance SiGe-based optical devices.

## Acknowledgments

This work was partly supported by the Strategic Information and Communications R&D Promotion Programme of the Ministry of Internal Affairs and Communications.